Measurements of Excitation Condition and Quantitative Mode Analysis in Optical Fibers

HIROSHI SHIGESAWA, MEMBER, IEEE, TOYOKI MATSUO, AND KEI TAKIYAMA, MEMBER, IEEE

***Abstract*—The purpose of this paper is to describe an accurate method for determining the modal-power distribution along optical fibers and also to present a technique for measuring the launching conditions produced by an input laser beam. Experimental results demonstrate both the accuracy and the effectiveness of those methods for investigating the transmission characteristics of optical waveguides. Various factors having an important influence upon the accuracy are discussed, and appropriate methods for minimizing the systematic errors also are presented.**

I. Introduction

IN THIS PAPER, we present an analytical method for measuring the modal-power distribution at the output end of an optical fiber. Instead of the mode selection technique proposed by Kapany *et al.* [1], we make an interferometric recording of the far-field distribution at the output of a fiber and then obtain the complex-field distribution just at the output end of a fiber by numerically analyzing this recording. Our method can be applied to obtain the modal powers in the propagating modes.

Following improvements in the fabricating techniques for optical fibers, multimode fibers with little mode conversions over several hundred meters have been produced. In such glass fibers, the modal-power distribution at the output end will be intimately related to the launching condition produced by an input laser beam. Thus the measurement of launching conditions becomes one of the techniques necessary for the study of fiber characteristics; a technique for measuring launching conditions characterized physically by three parameters is presented.

In addition, various factors having an important influence upon the accuracy are also discussed with methods of minimizing the systematic errors.

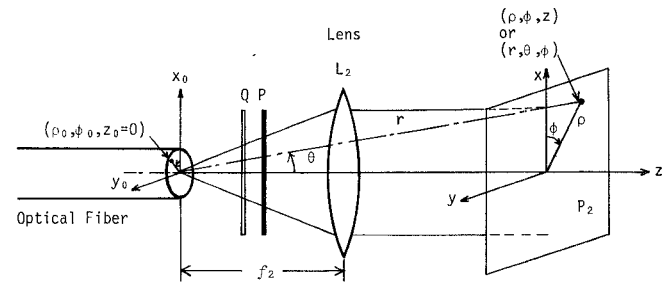

Fig. 1. Diffraction geometry for the mode analysis. (Q is the quarter-wave plate, P is the polarizer, and P_2 is the observation plane.)

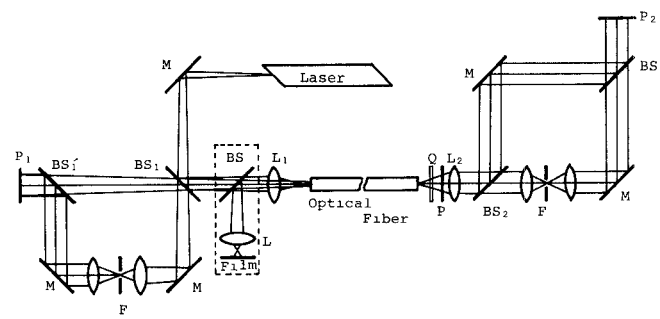

Fig. 2. Experimental arrangement for measuring the launching parameters and for the mode analysis. (BSα is the beam splitter, F is the dc spatial filter, Lα is the lens, M is the mirror, Pα is the observation plane, P is the polarizer, and Q is the quarter-wave plate.) This schematic shows the arrangement for the general use. When the LP components are concerned, the quarter-wave plate Q should be removed, and only a polarizer P will be used to select one of the LP components, while both Q and P are utilized to transform one of circular components into LP components when the circularly polarized components are concerned.

II. Principle of Measurements

A. Method of Quantitative Mode Analysis

For the mode analysis, let us consider the schematic as shown in Fig. 1 in which a definition for both spherical (r,θ,ϕ) and cylindrical (ρ,ϕ,z) coordinates is introduced. The origin of these coordinates is on the center of the exit end of a fiber, and the negative z axis is coincident with the axis of the fiber. As seen from the practical system of Fig. 2, the experimental setup will be modified and improved without loss of the theoretical foundation described in this section. As seen later, the present method has some analogy in part with the technique developed in the microwave region. As is well known, the measurement of the amplitude and phase distributions of the vector field on the cross section of a waveguide plays an important part in the quantitative mode analysis, and such a measurement will be performed easily by means of a probe detector in the microwave region. However, it is quite difficult, in the optical region, to measure the complex amplitude distribution in such a manner. Then a method applicable to the optical field will be, first, to decompose the field into two orthogonally polarized com-

Manuscript received May 5, 1978; revised July 31, 1978. This work was supported in part by the Ministry of Education, Science, and Culture, Japan, under a Scientific Research Grant-In-Aid, Grant 221737, Special Project Research, "Optical Guided-Wave Electronics," 1977.

The authors are with the Department of Electronics, Doshisha University, Kyoto, 602, Japan.

0018-9480/78/1200-0992$00.75 ©1978 IEEE

ponents $E_{\pm}$ which can be transformed easily into linearly polarized fields and, then, to apply an interferometric measurement of $E_{\pm}$ to obtain those complex amplitude distributions. For this purpose, the circularly polarized components will be used as the effective ones when the transmitted field is expressed by the linear combination of the TE, TM, HE, and EH modes, while linearly polarized (LP) components [2] are also useful in a weakly guiding fiber when the delay time of the modes' propagation is the main concern. In this paper, the treatment due to the LP modes is employed, and eigenmodes decomposed into two orthogonal components are denoted by the electric field $e_{\pm(n,m)}$ and the magnetic field $h_{\pm(n,m)} = e_{\pm(n,m)}/Z_{\pm(n,m)}$, where $Z_{\pm(n,m)}$'s indicate the characteristic parameters that have the dimension of impedance [1] and are peculiar to waveguides. In the above expressions, the subscripts $\pm$ show the vertically and horizontally polarized components, respectively, and the n and m indicate the azimuthal and radial order numbers of a mode, respectively. The alternative treatment of employing circular components was also adopted and has been presented in [3].

By referring to both the diffraction geometry of Fig. 1 and the mathematical treatments described in [1, ch. 6], we can express the Fraunhofer fields $E_{\pm}$ in terms of the inverse Fourier transform (F^{-1}) of $e_{\pm(n,m)}$ as follows.

$$E_{\pm}(\rho,\phi) = -\frac{i}{2\lambda f_2}\sum_n\sum_m \eta_{\pm(n,m)} A_{\pm(n,m)} F^{-1}[e_{\pm(n,m)}] \tag{1}$$

where $A_{\pm(n,m)}$'s are the modal amplitudes to be measured and f_2 denotes the focal length of lens L_2 which transforms the θ components of the field vector into ρ components perpendicular to the optical axis. In (1),

$$\eta_{\pm(n,m)} = \left\{\sqrt{\mu_0/\epsilon_0}\,/Z_{\pm(n,m)}\right\} + i \tag{2}$$

and is a complex constant peculiar to each mode. However, $\eta_{\pm(n,m)}$ may be regarded almost as a constant independent of (n,m) for modes far from cutoff. Thus, if we can measure experimentally the complex amplitude distribution of $E_{\pm}$, the modal amplitudes $A_{\pm(n,m)}$'s may be obtained approximately by introducing the orthogonality condition of $e_{\pm(n,m)}$ into the Fourier transform of $E_{\pm}$ as follows.

$$A_{\pm(n,m)} = \int_0^{2\pi}\int_0^{\infty} F[E_{\pm}]\, e^*_{\pm(n,m)} \rho_0 d\rho_0 d\phi_0 / \eta_{\pm(n.m)} \tag{3}$$

where the asterisk * denotes the complex conjugate and

$$F[E_{\pm}] = \int_0^{2\pi}\int_0^{\infty} E_{\pm}(\rho,\phi) \cdot \exp\left[-i\frac{k}{f_2}\rho_0\rho\cos(\phi_0-\phi)\right]\rho d\rho d\phi. \tag{4}$$

The calculation of (3), however, is not practical in the case of optical fibers because the modal eigenfunctions $e_{\pm(n,m)}$ extend to infinity in the ρ_0 direction. Then, we should introduce some effective approximations for $e_{\pm}$ when we calculate (3) numerically. One of them will be to truncate $e_{\pm(n,m)}$ at a finite radius, say a', and to approximate as $e_{\pm(n,m)} \simeq 0$ for $\rho_0 \geqslant a'$. This is discussed in [3].

B. Measurement Technique of Complex Amplitude Distribution

By using (3) together with the measured Fraunhofer field $E_{\pm}$, one can obtain the modal-power distribution transmitted through a fiber. In order to measure $E_{\pm}$ which may be expressed as $|E_{\pm}|\cdot\exp(i\Phi_{\pm})$, the Mach–Zehnder interferometer-like arrangement on the right-hand side of Fig. 2 is used where the polarizer P is placed immediately behind the exit end of a fiber to select one of two orthogonally polarized components. (Fig. 2 shows the arrangement for the general use, and the quarter-wave plate Q should be removed in this case.) After selecting this field, the vertically polarized component E_+ is collimated by the lens L_2. The selected field is then split at a beam splitter BS_2, and one of the components is transmitted directly to yield E_+ itself on the plane P_2, while the other in the lower arm of the interferometer is used as a reference wave R after passing through a dc spatial filter. These are recombined at another beam splitter BS_2' to yield the desired interference patterns on the plane P_2. In addition, the field E_+ also is made to interfere with another reference wave R' of which the phase is advanced by $\pi/2$ rad with respect to R. Consequently, the recorded patterns, i.e., $|E_+ + R|^2$, $|E_+ + R'|^2$, $|E_+|^2$, $|R|^2$, and $|R'|^2$ are then analyzed to obtain both the amplitude $|E_+|$ and phase Φ_+ of E_+. Similarly, one can obtain both the amplitude and phase of the horizontally polarized component E_- when the polarizer P is rotated by 90°. Moreover, if each modal amplitude of the TE, TM, HE, and EH modes is required, the field on the exit end of a fiber should be decomposed into two circular components, and then it will be effective to introduce a quarter-wave plate Q between the exit end of a fiber and P as shown in Fig. 2. This method has been applied [3] to obtain the modal-power distribution in a step-index multimode fiber.

C. Method for Measuring the Launching Condition

When a laser beam is launched into a fiber, there is always a reflection at the input plane of a fiber which produces the far-field distribution associated with the launching condition. The analysis of the reflected field will result in a method for measuring the launching condition. The diffraction geometry employed in the analysis is shown in Fig. 3, in which an input Gaussian beam excites a fiber through a launching lens L_1. The launching condition may be represented dominantly by the physical parameters such as the tilt angles γ, δ of the fiber axis and the axial mismatch a of an input beam as denoted schematically in the figure. Of course, both the intensity distribution of the launching beam and its center coordinates (x_c, y_c) on the input plane of a fiber become addi-

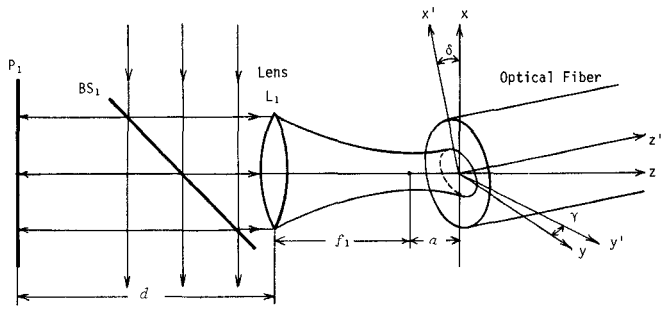

Fig. 3. Diffraction geometry for measuring the launching conditions and definition of launching parameters. (P_1 is the observation plane, γ,δ are the tilt angles, and a is the axial mismatch of the beam waist.)

tional important parameters to define the launching condition perfectly. However, it seems difficult to deduce such additional parameters from the analysis of the reflected field; we need another method, which is described later, to be employed in our experiments.

Now, by the reasonable approximations of small angles for γ,δ and homogeneous reflectivity across the input plane of a fiber, it may be shown that the reflected beam yields the field $U(x_i,y_i)$ on the plane P_1 as shown in the Appendix.

$$U(x_i,y_i)=g(x_i,y_i)\cdot\exp\left\{i\frac{ka}{f_1^2-2a(d-f_1)}\left[(x_i+f_1\delta)^2+(y_i+f_1\gamma)^2\right]\right\} \quad (5)$$

where the complex amplitude $g(x_i,y_i)$ is a smooth function on the plane P_1, f_1 is the focal length of the lens L_1, and also d indicates the distance from L_1 to P_1. Equation (5) is the result obtained by considering the wave propagation of the reflected beam toward the negative z axis and the phase transformation produced by L_1 and also succeeding Fresnel diffractions. In these calculations, the numerical orders of 10^7 (1/m) for k, 10^{-5} (m) for the minimum spot size ω_0 of an input beam, and 10^{-2} (m) for f_1 are assumed to simplify the diffraction integral.

Now, by making the interference pattern between the field $U(x_i,y_i)$ and a homogeneous plane wave, one can observe an off-axis Airy-like pattern on the plane P_1. As seen from (5), the center coordinates (x_{ic},y_{ic}) are related to the tilt angles γ,δ and are given as follows.

$$\delta=-x_{ic}/f_1 \quad \gamma=-y_{ic}/f_1. \quad (6)$$

On the other hand, the axial mismatch a is related to the radius of maximum brightness in that pattern and is derived from the difference of radii of successive maxima (r_{n+1} and r_n) as follows.

$$a=\lambda f_1^2\left[2\lambda(d-f_1)-\left(r_{n+1}^2-r_n^2\right)\right]. \quad (7)$$

D. Measurement Technique for Launching Condition

To obtain the launching parameters, the Mach–Zehnder interferometer-like arrangement in the left-hand side of Fig. 2 is used where the output beam from a laser is split at a beam splitter BS_1 and one of these excites a fiber through a launching lens L_1 in the same fashion as shown in Fig. 3, while the other, after generating a homogeneous plane wave by means of a dc spatial filter in the lower arm of the interferometer, reaches the plane P_1 as a reference wave. The reflection of the launching beam at the input plane of a fiber produces the far-field distribution of (5) across the plane P_1. These waves interfere and produce an off-axis Airy-like pattern as discussed in the previous section. In addition, a microscope-like arrangement enclosed by the dashed line in Fig. 2 is used to observe directly the intensity distribution of the launching beam and its center coordinates (x_c,y_c) in the input plane of a fiber.

III. Experiments and Discussions

To examine the relations between the launching condition and the modal-power distribution, several experiments have been performed by means of the present methods. Fig. 2 shows the experimental setup having a better stability in comparison with the interferometer of [3]. A SELFOC fiber was used for a test; the details of the fiber are as follows: the maximum refractive index on the fiber axis is 1.54, the quasi-core diameter is 35 μm, the cladding diameter is 200 μm, the refractive index of cladding is 1.525, and the length of the fiber is 1 m. To perform the mode analysis, the eigenmode for a SELFOC fiber should be expressed in an analytic function even though the graded index variation is truncated by the cladding with a constant index. However, we have not yet found proper analytic mode functions except for the fiber having a quadratic index variation without cladding, the modal functions of which may be successfully introduced so long as only the modes far from cutoff are considered in our SELFOC fiber. Several kinds of interference patterns at $\lambda=0.633$ μm are observed on both planes P_1 and P_2. Each of them is recorded rapidly on the image storage vacuum tube through a TV camera, and the sampled data are stored in a disk memory of a processing computer at a moderate speed. These instrumentations for automatic measurements and the software for data processing to obtain the desired results are interesting problems, but these are beyond the scope of this paper and will be discussed in a future publication.

In the first step of our experiments, the output beam from an He–Ne laser has been analyzed to confirm the validity of our method of mode analysis. For this purpose, the optical fiber in Fig. 2 is replaced with a laser which has a slight and parallel offset in both axes of laser mirrors [3]. In this case, the optical field is characterized only by a linearly polarized component, say, the vertically polarized component, and the treatment due to the TEM_{nm} modes is then employed. Table I shows the obtained result which informs us that the significant higher order modes produced in the laser cavity are TEM_{n0} modes ($n\neq 0$). From the physical considerations, it will be derived that the higher order modes in the azimuthal

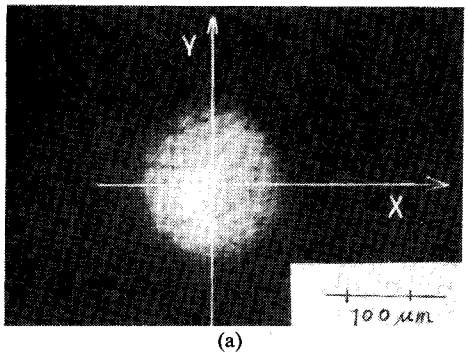

(a)

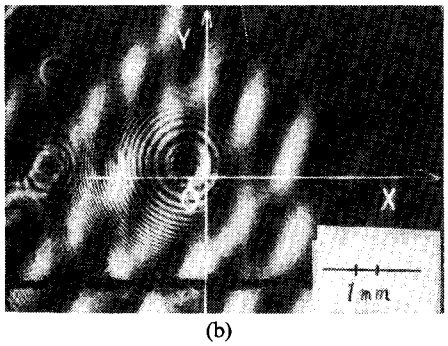

(b)

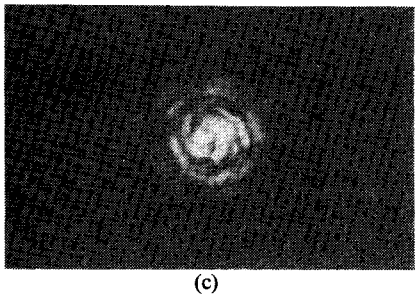

(c)

Fig. 4. Examples of the observed patterns of (a) the intensity distribution of the launching beam on the input plane, (b) the interference pattern observed on the plane P_1, and (c) the intensity distribution of the transmitted field on the output plane of a fiber.

TABLE I
RESULTS OBTAINED IN THE EXPERIMENT FOR AN OUTPUT OF A LASER HAVING A SLIGHT OFFSET OF MIRRORS ($|A_{nm}|$ ARE NORMALIZED BY THE MAXIMUM ONE)

Mode	|Anm|
TEM 0 0	1.00
0 1	0.29
0 2	0.02
0 3	0.03
1 0	0.42
1 1	0.09
1 2	0.04
1 3	0.02
2 0	0.27
2 1	0.04
2 2	0.04
2 3	0.01
3 0	0.19
3 1	0.07
3 2	0.03
3 3	0.02

order number n are produced dominantly by the slight offset of axes of laser mirrors. Although the numerical considerations have not yet been done, this situation fits the results obtained in Table I well.

Next, several experiments have been performed by using a SELFOC fiber, and a few results are summarized in Tables II–IV. Fig. 4 shows the examples of photographic recordings of the field intensity distributions and the interference fringes observed in the experiment for Table III. All of these results are obtained for the input beam having $\omega_0 = 5.2$ μm which coincides with the eigenspot size of a SELFOC fiber. As for the results of Tables II and III, the tilt angles γ, δ are almost identical with each other, and there are differences of the launching parameters in both the axial mismatch a and the off-axial center (x_c, y_c) of the input beam. It has been shown in [6] that, although the axial mismatch a has a tendency to excite higher order modes in the radial order number m, the a of between -200 and 200 μm causes the amplitude deviation of at most 15 percent in each excited mode by $a = 0$.

Then we should understand that the principal causes of the difference between both results of Tables II and III are not owing to the axial mismatch a but owing to the off-axial center of the input beam on the input plane of a fiber. Moreover, it will also be derived from [6] that the input beam having an off-axial center on the input plane excites mainly the higher order modes in the azimuthal order number n when the off-axial center $r_c = \sqrt{x_c^2 + y_c^2}$ exceeds ω_0. Indeed, this phenomenon interprets well the result of Table II in which r_c is 1.6 times as large as that of Table III, but the full arguments based on the numerical calculations have not yet been given successfully. On the other hand, it will be clear in Tables III and IV that the launching conditions are almost the same except for the tilt angle δ. Thus these results suggest that the higher order modes in the radial order number are principally excited as the tilt angles become larger. This matches again the discussions in [6]. Consequently, our results suggest that the coupling of an input beam into the higher order propagation modes is less affected by the incomplete launching having an axial mismatch a than by that having both tilt angles γ, δ and the off-axial center (x_c, y_c) of the input beam on the input plane of a fiber.

To obtain the accurate results in the mode analysis, special attention should be paid, at least, to the following three points: 1) the allowable separation Λ between samples for the recorded patterns, 2) the recovery of original data for $E_{\pm}$ from the sampled data $E'_{\pm}$, and 3) the minimum radius R_m for the lens L_2 to give no influences on the radiated field.

For the first problem, it may be roughly assumed that the field at the output end of a fiber is confined in and near the quasi-core region for well-guided modes, and thus the field $E_{\pm}$ will be regarded as a spatially band-limited function even though the lens L_2 has a sufficiently large aperture. Then the Nyquist condition defines the sufficient separation Λ as $\lambda f_2 / 2 r_0$, where r_0 is the quasi-core radius. In our case, this separation becomes about 1.26 mm, while the electronic sampler has been operated with 0.9-mm spacing in the experiments.

In the second problem, the sampled data $E'_{\pm}$ are convolved, in our case, with the window function of an

TABLE II
TYPICAL RESULTS OBTAINED IN THE EXPERIMENTS FOR A SELFOC FIBER (γ, δ IN DEGREES AND a, x_c, y_c IN MILLIMETERS AND $|A_{nm}|$ ARE NORMALIZED BY THE MAXIMUM ONE)

δ=-4.01 , γ= 1.92
a= 0.0 , x_c=-0.03
y_c= 0.02

Mode	|Anm|
LP 0 3	1.00
2 1	0.90
1 1	0.71
3 1	0.50
2 3	0.49
0 8	0.44
0 1	0.44
0 4	0.43
0 7	0.42
1 2	0.41
0 5	0.41
0 2	0.36
1 6	0.36
2 2	0.36
1 4	0.34

TABLE III
TYPICAL RESULTS OBTAINED IN THE EXPERIMENTS FOR A SELFOC FIBER (γ, δ IN DEGREES AND a, x_c, y_c IN MILLIMETERS AND $|A_{nm}|$ ARE NORMALIZED BY THE MAXIMUM ONE)

δ= 4.32 , γ=-2.07
a=-0.12 , x_c=-0.02
y_c=-0.01

Mode	|Anm|
LP 1 1	1.00
0 1	0.72
1 5	0.60
1 2	0.56
0 5	0.43
0 4	0.39
1 4	0.37
1 3	0.32
3 1	0.30
1 6	0.29
0 7	0.23
0 8	0.23
2 3	0.22
2 1	0.21
2 4	0.21

TABLE IV
TYPICAL RESULTS OBTAINED IN THE EXPERIMENTS FOR A SELFOC FIBER (γ, δ IN DEGREES AND a, x_c, y_c IN MILLIMETERS AND $|A_{nm}|$ ARE NORMALIZED BY THE MAXIMUM ONE)

δ= 5.12 , γ=-2.14
a=-0.13 , x_c=-0.02
y_c=-0.01

Mode	|Anm|
LP 1 3	1.00
1 1	0.91
1 2	0.74
0 7	0.70
010	0.67
0 5	0.61
0 4	0.51
0 2	0.49
3 1	0.48
2 2	0.44
2 1	0.38
1 4	0.32
2 5	0.32
0 1	0.30
1 6	0.29

electronic sampler, i.e., the finite radius of the beam spot of a TV camera. Then the desired original data $E_{\pm}$ may be obtained by applying the deconvolution technique successfully developed in [4], [5].

Finally, the minimum radius R_m for the lens L_2 may be derived from the numerical aperture (NA) of a fiber. Supposing that the radiation field of the highest order mode in a fiber is concentrated in a cone with the apex angle Θ_m, it is obvious that the relation $R_m \simeq f_2 \Theta_m$ should hold. In our case, the fiber NA is about 0.21 and the apex angle Θ_m is about 12.5°. Then R_m is given by 15 mm when a lens having $f_2 = 70$ mm is used, and so the lens with a radius of 25 mm is enough for our experiments.

Furthermore, there are some residual factors having an influence on the errors. These are, for example, the reduced visibility in the interference patterns produced by the partial coherency of a laser and the misalignment of interferometers. These problems are in common with the ordinary laser interferometers, and the counterplans considered in those fields will become effective.

IV. Conclusion

In light transmission through a multimode fiber with little mode conversion, there exists a modal-power distribution which is intimately related to the launching condition produced by an input laser beam, even for the field after transmission over several hundred meters. This paper has described methods for quantitative mode analysis and for measuring the launching condition. Our method of mode analysis is indeed rather elaborate, and there are some other simpler but incomplete methods, e.g., the one given by [7]. The last method will not be effective when there are many propagating modes having close eigenvalues. Our methods may be applied effectively to examine the characteristics of mode conversion in fiber splicings and connectors and also to obtain the proper impulse response independent of the launching condition. We are currently working to improve the arrangement for these studies and to discuss the accuracy of the techniques proposed here in more detail.

V. Appendix
Derivation of (5)

Let us simplify the diffraction geometry of Fig. 3 by ignoring the Gaussian spreading of an input beam on the focal plane of lens L_1. Then, under the assumptions of the small angles γ, δ and the homogeneous reflectivity across the input plane of a fiber, the reflected wave will be regarded as a spherical wave radiated from the point source at the point given by

$$x_s \simeq 2a\delta \quad y_s \simeq 2a\gamma \quad z_s \simeq a. \tag{A1}$$

This point will be obtained from the mirror image of the focal point about the input plane of a fiber as shown in Fig. 5. If the paraxial approximation is adopted, the reflected field immediately in front of a lens L_1 of focal length f_1 becomes

$$U_L(x_0, y_0) = \text{const.} \exp\left\{ -i \frac{k}{2d_s} \left[(x_0 - x_s)^2 + (y_0 - y_s)^2 \right] \right\} \tag{A2}$$

where

$$d_s = f + 2a \tag{A3}$$

and const indicates an arbitrary complex constant having no influence on the result in any significant way.

To find the distribution $U(x_i, y_i)$ of the field amplitude across the plane P_1, both the transformation due to L_1

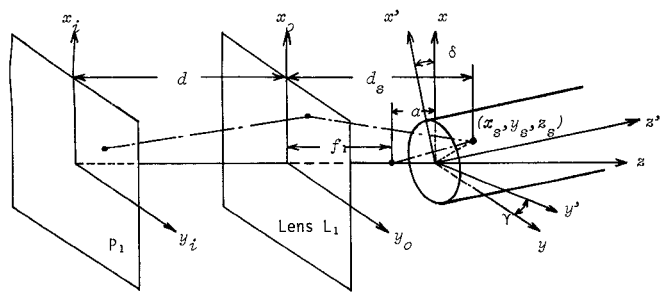

Fig. 5. Diffraction geometry for the analysis of a reflected wave from an input plane of a fiber. (x_s, y_s, z_s are the coordinates for the assumed point source and P_1 is the observation plane.)

$(\exp[ik(x_0^2+y_0^2)/2f_1])$ and the succeeding Fresnel diffraction accounting for propagation over the distance d are applied to $U_L(x_0,y_0)$. Thus we obtain formally

$$U(x_i,y_i) \simeq \text{const.} \int\int_{-\infty}^{+\infty} U_L(x_0,y_0) \exp\left\{ i\frac{k}{2f_1}(x_0^2+y_0^2) \right\} \cdot \exp\left\{ -i\frac{k}{2d}\left[(x_i-x_0)^2+(y_i-y_0)^2\right] \right\} dx_0 dy_0. \tag{A4}$$

After performing the integrations in (A4), we obtain

$$U(x_i,y_i) = \text{const.} \exp\left\{ i\frac{k}{2} \cdot \frac{(d_s-f_1)}{(f_1 d_s + f_1 d_s - d d_s)} \cdot \left[\left(x_i + \frac{f_1}{(d_s-f_1)} x_s \right)^2 + \left(y_i + \frac{f_1}{(d_s-f_1)} y_s \right)^2 \right] \right\}. \tag{A5}$$

When the Gaussian spreading of an input beam at the focal point of L_1 is taken into account, we should replace the spherical wave radiated from the point source at (x_s,y_s,z_s) with the Gaussian beam having the same characteristic parameters as those of the input beam. In this case, the mathematical treatment is somewhat complicated. However, if the numerical orders for k, ω_0, and f_1 as described in Section II-C are considered, the Gaussian spreading has no significant modification in the result of (A5) except for the replacement of const. in (A5) with a smooth function of (x_i,y_i). The explicit form of this function, denoted as $g(x_i,y_i)$ in (5), is quite tedious and will be omitted here because it has no significant effects when the launching parameters are concerned. Consequently, we can obtain (5) by introducing (A1) and (A3), into (A5).

References

[1] N. S. Kapany and J. J. Burke, *Optical Waveguides*. New York: Academic Press, 1972, ch. 6.

[2] D. Gloge, "Weakly guiding fibers," *Appl. Opt.*, vol. 10, pp. 2252–2258, Oct. 1971.

[3] T. Hirashima, H. Shigesawa, and K. Takiyama," Quantitative mode analysis in optical fibers," *Trans. IECE Japan*, vol. 59-C, pp. 258–260, Apr. 1976.

[4] H. Shigesawa, K. Takiyama, and M. Nishimura, "High-quality image reconstruction from double microwave holograms," *IEEE Trans. Microwave Theory Tech.*, vol. MTT-24, pp. 529–531, Apr. 1976.

[5] J. I. Harris, "Image evaluation and restoration," *J. Opt. Soc. Am.*, vol. 56, pp. 569–574, May 1969.

[6] Y. Yoda, H. Shigesawa, and K. Takiyama, "Mode excitation and impulse response in the multi-mode self-focusing fiber," *Science Eng. Rev. Doshisha Univ.*, vol. 18, pp. 253–270, Mar. 1978.

[7] M. Ikeda and H. Yoshikiyo, "Pulse separating in transmission characteristics of multimode graded index optical fibers," *Appl. Opt.*, vol. 15, pp. 1307–1312, May 1976.